Delayed [18F]-FDG PET Imaging Increases Diagnostic Performance and Reproducibility to Differentiate Recurrence of Brain Metastases From Radionecrosis

Hosameldin Otman, Julien Farce, Pierre Meneret, Xavier Palard-Novello, Pierre Jean Le Reste, Isabelle Lecouillard, Elodie Vauléon, Elodie Vauleon, Marion Chanchou, Beatrice Carsin Nicol, et al.

Title page

Article type: Original article

Title:

Delayed [^{18}F]-FDG PET imaging increases diagnostic performance and reproducibility to differentiate recurrence of brain metastases from radionecrosis

Authors:

Hosameldin OTMAN [1], Julien FARCE [2], Pierre MENERET [2], Xavier PALARD-NOVELLO [2,3], Pierre-Jean LE RESTE [4], Isabelle LECOUILLARD [5], Elodie VAULEON [6], Marion CHANCHOU [1,7], Beatrice CARSIN NICOL [8], Marc BERTAUX [9], Anne DEVILLERS [2], Denis MARIANO-GOULART [10], Florent CACHIN [1,7], Antoine GIRARD [2,3], Florence LE JEUNE [2,3]**

* These two authors contributed equally to this work and are co-last authors.

1. Department of Nuclear Medicine, Jean Perrin Center, Clermont-Ferrand, France

2. Department of Nuclear Medicine, Eugène Marquis Center, Rennes, France

3 INSERM, LTSI-UMR 1099, University of Rennes, Rennes, France

4. Department of Neurosurgery, Rennes University Hospital, Rennes, France

5. Department of Radiation Onclogy, Eugène Marquis Center, Rennes, France

6. Department of Medical Onclogy, Eugène Marquis Center, Rennes, France

7. INSERM U1240 « Imagerie moléculaire et stratégie théranostique », University of Clermont Auvergne, Clermont-Ferrand, France

8. Department of Neuroradiology, Rennes University Hospital, Rennes, France

9. Department of Nuclear Medicine, Foch hospital, Suresnes, France

10. Department of Nuclear Medicine. Montpellier University Hospital. PYMEDEXP, University of Montpellier, INSERM, CNRS

Corresponding Author:

Dr Antoine Girard (ORCID: 0000-0002-9472-9980)

Department of Nuclear Medicine, Centre Eugène Marquis, Avenue de la Bataille Flandres-Dunkerque, Rennes, France

Email: antoine.girard.89@gmail.com Phone: +33 2 99 25 30 00

Word count: Abstract: 249/250 Full: 4310/4500

Financial support: This study did not benefit from any funding

Short title: Delayed brain FDG PET detects recurrence

Conflict of interest disclosure statement: The authors have no potential conflicts of interest to disclose

Title page

Title:

Delayed [^{18}F]-FDG PET imaging increases diagnostic performance and reproducibility to differentiate recurrence of brain metastases from radionecrosis

Abstract

Purpose: Differentiating brain metastasis recurrence from radiation necrosis (RN) can be challenging during MRI follow-up after stereotactic radiotherapy. 2-deoxy-2-[^{18}F]fluoro-D-glucose ([^{18}F]-FDG) is the most available PET tracer, but standard images performed 30-60 minutes post-injection provide insufficient accuracy. We compared the diagnostic performance and interobserver agreement of [^{18}F]-FDG PET with delayed images (4-5h post-injection) to the ones provided by standard and dual-time-point imaging.

Materials and Methods: Consecutive patients referred for brain [^{18}F]-FDG PET after inconclusive MRI were retrospectively included between 2015 and 2020 in three centers. Two independent nuclear medicine physicians interpreted standard (visually), delayed (visually), and dual-time-point (semi-quantitatively) images, respectively. Adjudication was applied in case of discrepancy. The final diagnosis was confirmed histologically or after 6 months of MRI follow-up. Areas under receiver operating characteristics curves (AUC) were pairwise compared.

Results: Forty-eight lesions from 46 patients were analyzed. Primary tumors were mostly located in the lungs (57%) and breast (23%). The median delay between radiotherapy and PET was 15.7 months. The final diagnosis was tumor recurrence in 24/48 (50%) lesions, with histological confirmation in 19/48 (40%) lesions. Delayed images provided a larger AUC (0.88, 95% CI[0.75, 0.95]) than both standard (0.69, 95% CI[0.54, 0.81], p=0.0014) and dual-time-point imaging (0.77, 95% CI[0.63, 0.88], p=0.045), respectively. Interobserver agreement was almost perfect with delayed images (**K**=0.83), while moderate with both standard (**K**=0.48) and dual-time-point images (**K**=0.61).

Conclusions: [^{18}F]-FDG PET with delayed images is an accurate and reliable alternative to differentiate metastasis recurrence from RN in case of inconclusive MRI after brain stereotactic radiotherapy.

Keywords

[^{18}F]-FDG PET; brain metastases; radiation necrosis; positron emission tomography; radiation therapy

Full text

Introduction

Brain metastases are the most common cause of intracranial malignant tumors and can worsen the course of many types of cancers. Stereotactic radiotherapy (SRT) alone or after surgical resection is now a standard of care for patients with a limited number of secondary brain tumors.[1] Radiation necrosis (RN) is one of the most frequent radiation therapy adverse events. It can occur from 3 months to several years after the end of radiotherapy. The incidence rate of RN has been reported between 15% and 50% depending on several factors such as the radiotherapy modality, the total dose, the intracranial pathology, and the imaging modality used for diagnosis.[2] Differentiating RN from viable tumor tissue is of major importance since it impacts patient management and outcome. Surgery or SRT can be proposed for recurrent brain metastases, whereas RN management is symptomatic and commonly relies on steroids.[1]

Conventional MRI is the imaging method of reference during follow-up of brain metastases. Nevertheless, differentiating tumor recurrence from RN can often be challenging. The Response Assessment in Neuro-Oncology Brain Metastases (RANO-BM) stated that advanced imaging modalities such as perfusion-weighted imaging (PWI), MR spectroscopy, and PET are of interest to face this limitation.[3] In this setting, the RANO/PET working group recommended amino acid PET tracers because of their good diagnostic performance despite their low availability in clinical practice.[4] Conversely, 2-deoxy-2-[^{18}F]fluoro-D-glucose ([^{18}F]-FDG), which is the most widely used PET tracer in oncology, currently provides insufficient and variable diagnostic performance when used with standard protocols (brain images performed 30 to 60 minutes after tracer injection). The reported sensitivity of standard [^{18}F]-FDG ranges from 40% to 83% and its specificity ranges between 50% and 94%.[5-9] This limited diagnostic performance can be explained by a low tumor-to-brain ratio (TBR) since normal gray matter shows an intense and early physiological [^{18}F]-FDG uptake. To overcome this issue by maximizing the TBR, some authors performed additional delayed PET images 4 to 5 hours after [^{18}F]-FDG injection. With such protocols, [^{18}F]-FDG PET reached a sensitivity of 93%-95% and a specificity of 94%-100%.[10-11] Nevertheless, the limited amount of evidence supporting these results and the time-consuming aspect of dual-time point protocols hinder its widespread use in clinical practice. We hypothesized that delayed [^{18}F]-FDG PET images alone have a good diagnostic performance to differentiate recurrence of brain metastases from RN.

This study aimed to compare the diagnostic performance of standard, delayed, and dual-time-point [^{18}F]-FDG PET imaging to differentiate viable tumors from RN after radiotherapy of brain metastases, based on area under the receiver operator characteristic curves (AUC) and interobserver agreement.

Material and methods

Patients

In this retrospective multicentric study, a total of 59 consecutive patients (n = 61 lesions) referred for brain [^{18}F]-FDG PET to differentiate tumor progression from RN were retrospectively included between August 2015 and August 2020 in three French tertiary care centers. Inclusion criteria were as follows: having performed brain [^{18}F]-FDG PET with standard and delayed images following an inconclusive MRI revealing new or increasing contrast enhancement at least 3 months after the end of radiation therapy, being at least 18 years old, having previously received brain SRT for one or more metastatic lesions. Non-inclusion criteria were: having a primary tumor of the brain and [^{18}F]-FDG PET technically uninterpretable (corrupted data or missing delayed images). The exclusion criterion was the absence of reference standard available (defined below). For patients who underwent several brain [^{18}F]-FDG PETs over time, only the first one was analyzed. This study was approved by institutional ethical committees for each center. All the patients included were informed and did not object to participating in this study. This study was conducted following the principles outlined in the declaration of Helsinki. This report was written in accordance with the STARD guidance.[12]

[^{18}F]-FDG PET/CT protocol

Six hours of fasting and blood glucose level of less than 12 mM/L were required before intravenous injection of [^{18}F]-FDG (200 MBq). Patients were asked to rest and fast during at least the first hour after injection. Standard brain PET images were acquired after 30 to 60 minutes of rest after intravenous [^{18}F]-FDG injection. Delayed brain PET images started between 240 and 300 minutes post-injection (p.i.).[10,11] Patients were allowed to eat between the standard and late phase scans. Unenhanced CT scans were used for attenuation correction. PET images were performed on several PET/CT integrated systems. PET acquisition protocols and PET systems are detailed in **Supplementary Material**.

Reference standard

A composite criterion was used as a reference standard for differentiating viable tumors (recurrence and/or residual tumor) from pure RN (without viable neoplastic cells). A lesion was classified as a viable tumor if 1) a pathological analysis of a biopsy and/or resection specimen revealed neoplastic cells in this area within 6 months after [^{18}F]-FDG PET or 2) imaging follow-up revealed unequivocal progression within 6 months after [^{18}F]-FDG PET (i.e. significant increase of the size of contrast enhancement and/or appearance of neoangiogenesis). On the

contrary, a lesion was classified as RN without viable tumor cells if 1) a pathological analysis of a biopsy and/or resection specimen performed within 6 months after [^{18}F]-FDG PET revealed no neoplastic cells or 2) stabilization or shrinkage of contrast enhancement on MRI over a least 6 months without modification of anti-tumor treatment (the introduction of steroids or antiangiogenic agents was accepted).[13-15] Lesions were excluded from the analysis if they did not meet these criteria.

Image analysis

[^{18}F]-FDG PET images were registered and fused with the last contrast-enhanced T1-weighted MRI (that reported new or increasing contrast enhancement) and then visually and semi-quantitatively analyzed by two independent certified nuclear medicine physicians. In case of discrepancy between both raters regarding the diagnostic conclusion for each method respectively, adjudication was provided by a third nuclear medicine physician. For visual analysis, lesions were regarded as viable tumors if the [^{18}F]-FDG uptake intensity was higher than the contralateral normal gray matter on the same slice, respectively on standard and delayed images.[11] Otherwise, lesions were regarded as pure RN. The semi-quantitative dual-time point analysis was performed using the index over time of tumor-to-brain maximal standardized uptake values (SUVmax) ratios ($TBR = Lesion_{SUVmax} / Healthy\_contralateral\_gray\_matter_{SUVmax}$), as published by Horky, et al [$(TBR_{delayed} - TBR_{standard})/(TBR_{standard})$]. Based on this publication, lesions were individually considered as viable tumors if this index was > 0.19, and as RN in the opposite case.[10]

Statistical analysis

The analysis was performed with MedCalc® version 12.5.0.0 (Medcalc Software bvba, Ostend, Belgium). The distribution of continuous variables was described by the median associated with the interquartile range (IQR). AUC was calculated as the mean of the estimated sensitivity and specificity (based on the diagnostic conclusion of the consensus of readers, after adjudication) and pairwise compared with the Delong test. Interobserver agreement (between diagnostic conclusions of each of the two first readers, before adjudication) was calculated with the linear weighted Kappa and classified categorically.[16] The percentage of agreement was compared by using the Chi-squared test. TBR between standard and delayed images were compared with the Wilcoxon test. Two-tailed *p* values were considered statistically significant if < 0.05.

Results

Patients' characteristics

Out of fifty-nine patients, thirteen were excluded since they did not meet the reference standard: 4 were lost to follow-up, 7 died of extracerebral progression before reaching the reference standard, and 2 had treatment modification after [^{18}F]-FDG PET preventing reliable lesions classification (one received reirradiation, and the other one chemo- and targeted therapy, not allowing to categorize lesions as RN despite shrinking over time). Thus, 48 metastatic lesions of 46 patients (18 male and 28 female, median age 62y IQR[51, 67]) with various histologically-proven primary cancers were included in the final analysis (**Fig. 1**). Characteristics of patients and metastatic lesions included in the analysis are summarized in **Table 1**. The median time delay between MRI and PET was 25 days [IQR 17, 36]. All lesions were previously treated with SRT, either upfront in 35 lesions (73%) or after resection surgery in 13 lesions (27%). The median time delay between radiotherapy and PET was 15.7 months [IQR 9.4, 24.0]. According to the reference standard, 24 of 48 lesions (50%) were tumor recurrence and 24 (50%) were pure RN. The reference standard was based on pathological analysis in 19 (40%) of patients.

Comparison of diagnostic performance

Visual interpretation of delayed images only provided a significantly larger AUC (0.88, 95% CI [0.75, 0.95]) than both visual interpretation of standard images (0.69, 95% CI [0.54, 0.81], p = 0.0014) and semiquantitative analysis of dual-time-point imaging (0.77, 95% CI [0.63, 0.88], p = 0.045), respectively. Similarly, sensitivity was significantly higher with visual interpretation of delayed PET images (0.83, 95% CI [0.63, 0.95]) than with visual interpretation of standard images (0.46, 95% CI [0.26, 0.67], p = 0.001) and with semi-quantitative analysis of dual-time-point imaging (0.63, 95% CI [0.41, 0.81], p = 0.022). There was no statistically significant difference between AUC and sensitivity obtained with dual-time-point imaging and standard images (p = 0.24 and p = 0.21, respectively). In contrast, specificity was identical with each of the three imaging strategies (0.92, 95% CI [0.73, 0.99], p = 1.00 for each pairwise comparison). Details of diagnostic performance are presented in **Table 2**. Examples of standard and delayed [^{18}F]-FDG PET images of tumor recurrences and RN are presented in **Fig. 2**.

Interobserver agreement

The interobserver agreement of visual interpretation of delayed [^{18}F]-FDG PET images was almost perfect, with a Kappa coefficient of 0.83 (95% CI[0.68, 0.99]), while it was moderate with both standard images (0.48, 95% CI[0.23, 0.74]) and dual-time point semi-quantitative analysis (0.61, 95% CI[0.38, 0.84]). The percentage of concordance was significantly higher with delayed [^{18}F]-FDG PET images (92%) compared to standard images (77%, p = 0.04). In contrast, there was no statistically significant difference of percentage of concordance

between dual-time point analysis (80%) and delayed images (p = 0.12), nor between dual-time point analysis and standard images (p = 0.63), respectively.

Evolution of TBR over time

TBR of viable tumors was higher on delayed [^{18}F]-FDG PET images (1.37 IQR[1.02, 1.84]) than on standard images (0.96 IQR[0.87, 1.18], p < 0.0001). In contrast, TBR of pure RN did not differ significantly between standard (0.60 IQR[0.48, 0.77]) and delayed images (0.64 IQR[0.47, 0.78], p = 0.94) (**Fig. 3**). The increase of the TBR value between standard and delayed images was significantly higher for viable tumors (0.37 IQR[0.13, 0.69]) than for RN (0.02 IQR[-0.08, 0.09]). Only one lesion labeled positive on standard [^{18}F]-FDG PET images was reclassified as negative based on delayed images. This latter was concluded to be RN according to follow-up.

Discussion

Differentiating tumor recurrence from RN can be challenging during MRI follow-up of brain metastases treated with SRT. While histopathology remains the gold standard, accurate non-invasive diagnostic tools are needed to avoid the potential morbidity related to surgical biopsy or resection. PET is currently an imaging method of choice to complete inconclusive MRI in this indication.[1] Standard [^{18}F]-FDG PET (with images performed 30 to 60 min p.i.) has shown insufficient diagnostic performance.[4] In the present study from three different centers, optimized [^{18}F]-FDG PET protocols with delayed images (4 to 5 hours p.i.) alone provided higher diagnostic performance than standard [^{18}F]-FDG PET, with a better (almost perfect) interobserver agreement.

The RANO-BM working group cited [^{18}F]-FDG and/or radiolabeled amino acid PET as useful imaging methods to complement MRI in order to differentiate tumor recurrence from RN. Increased [^{18}F]-FDG (radiolabeled glucose analog) uptake is commonly seen in proliferating tumor cells due to an increased expression of glucose transporters and the enzyme hexokinase.[17] [^{18}F]-FDG is currently the most widely available and one of the less expensive PET tracers, but its performance when performed 30-60 p.i. is weak and fickle. Reported sensitivity ranges between 40-83% and specificity between 50-94% (in series regarding metastases only, with at least 20% of histological confirmation).[7-9,18] This limited diagnostic value is mainly due to the high and early physiological [^{18}F]-FDG uptake of the normal gray matter, decreasing the detectability of lesions.[19] In the present study, the median TBR of viable tumors was 0.96 on standard images. Moreover, inflammation related to RN can show a moderate early [^{18}F]-FDG uptake that is difficult to distinguish from viable tumor tissue. Because of this limitation, the RANO/PET working group as well as the joint guidelines from the European Association of

Neuro-Oncology (EANO) and the European Society for Medical Oncology- (ESMO) stated that PET with radiolabeled amino acids, such as [^{11}C]-methyl-L-methionine (MET), O-(2-[^{18}F]fluoroethyl)-L-tyrosine (FET), and 3,4-dihydroxy-6-[^{18}F]-fluoro-L-phenylalanine (F-DOPA), should be preferred in this indication.[4,20,21] These tracers' uptake is related to large amino acid transporters which are overexpressed in tumor tissue but show low uptake in the normal brain.[22-24] Reported diagnostic performance of amino acids PET is high and reproducible with sensitivity ranging between 74%-90%, and specificity between 75%-100% (in series regarding metastases only, with at least 20% of histological confirmation).[9,25-31] Nevertheless, radiolabeled amino acids are much more expensive than [^{18}F]-FDG, and their availability is more restricted worldwide even in some areas of developed countries.[32] Furthermore, amino acid PET tracers are not FDA approved for imaging brain metastases in several countries including the USA and France. To overcome these issues, optimized [^{18}F]-FDG PET protocols including delayed images performed 4 to 5 hours after injection (alone or dual-time-point) are emerging in clinical practice. Such protocols enable maximization of the lesion-to-background ratio in tumor recurrence, since [^{18}F]-FDG continuously increases in viable tumors over time while it washes out the normal brain and inflammatory tissue.[19] To date, two studies investigating such delayed [^{18}F]-FDG PET images have been published, revealing promising results with 93%-95% sensitivity and 94%-100% specificity.[10,11] Our results are in the line with these data, with 83% sensitivity and 92% specificity provided by visual analysis of delayed [^{18}F]-FDG PET images alone, significantly higher than with respectively standard and dual-time-point [^{18}F]-FDG PET. Such results can be explained by the significant increase of TBR over time for viable metastases but not for RN, which significantly enhanced the sensitivity without loss of specificity. Performance values obtained with delayed [^{18}F]-FDG PET images are in the same range as those reported in the literature with amino acid PET.

In our study, delayed [^{18}F]-FDG PET images alone provided higher diagnostic performance than both standard and dual-time-point images, with a simple visual interpretation and an almost perfect interobserver agreement. Thus, we suggest that a *delayed brain PET images only* protocol could be used in this setting as it would be time-saving and facilitate applicability in clinical routine. In the specific case when an extracranial evaluation is required by a whole-body PET at 60 min p.i., if standard brain images performed concomitantly reveal increased lesion [^{18}F]-FDG uptake, then delayed brain PET images can be considered unnecessary since standard images alone have a similarly high specificity (92%).

A direct comparison between delayed [^{18}F]-FDG PET images and multi-parametric MRI in this setting would be of interest as MRI is the cornerstone imaging modality for brain metastasis diagnosis and monitoring. PWI is the

most commonly advanced MRI technique used in clinical practice to distinguish tumor recurrence from RN. Relative cerebral blood volume is generally increased in viable tumor tissue due to neoangiogenesis but optimal cut-off levels are difficult to determine and diagnostic performance varies considerably.[20,33] In a recent meta-analysis, pooled sensitivity and specificity of dynamic susceptibility contrast PWI were 82% (95% CI[71%, 89%]) and 81% (95% CI[64%, 91%]), respectively, with heterogeneous interpretation criteria.[34] A few studies suggested that MR spectroscopy might be of interest to differentiate brain metastasis recurrence from RN, but poor sensitivity of approximately 33% (particularly for small lesions) and heterogeneous interpretation criteria hamper its widespread use.[33,35,36]

The present study had some limitations. The retrospective design is the first of them. Second, as for most of the studies published in the field, the final diagnosis was based on histology for less than a half (40%) of patients.[7-10,25-30] Finally, in this study in a real-life setting, thirteen patients had to be excluded because they did not meet the strict reference standard. Thus, patients included in the final analysis had a reliable final diagnosis.

Conclusion

[^{18}F]-FDG PET with delayed images alone provides very good diagnostic performances, better than those obtained with both standard and dual-time-point [^{18}F]-FDG PET, with an almost perfect inter-rater agreement. This technique requires only one PET acquisition and relies on the most widely available and one of the least expensive PET tracers. Thus, [^{18}F]-FDG PET with delayed images alone should be considered in everyday practice to complete inconclusive morphological MRI to differentiate brain metastasis recurrence from radionecrosis. Head-to-head analyses are still to be performed to confirm the non-inferiority of delayed [^{18}F]-FDG PET compared to amino acid PET and PWI.

References

1. Soffietti R, Abacioglu U, Baumert B, et al. Diagnosis and treatment of brain metastases from solid tumors: guidelines from the European Association of Neuro-Oncology (EANO). *Neuro Oncol*. 2017;19:162–74.

2. Ali FS, Arevalo O, Zorofchian S, et al. Cerebral Radiation Necrosis: Incidence, Pathogenesis, Diagnostic Challenges, and Future Opportunities. *Curr Oncol Rep*. 2019;21:66.

3. Lin NU, Lee EQ, Aoyama H, et al. Response assessment criteria for brain metastases: proposal from the RANO group. *The Lancet Oncology*. 2015;16:e270–8.

4. Galldiks N, Langen K-J, Albert NL, et al. PET imaging in patients with brain metastasis-report of the RANO/PET group. *Neuro Oncol*. 2019;21:585–95.

5. Li H, Deng L, Bai HX, Sun J, Cao Y, et al. Diagnostic Accuracy of Amino Acid and FDG-PET in Differentiating Brain Metastasis Recurrence from Radionecrosis after Radiotherapy: A Systematic Review and Meta-Analysis. *AJNR Am J Neuroradiol*. 2018;39:280–8.

6. Galldiks N, Lohmann P, Albert NL, et al. Current status of PET imaging in neuro-oncology. *Neuro-Oncology* Advances. 2019;1:vdz010.

7. Belohlávek O, Simonová G, Kantorová I, et al. Brain metastases after stereotactic radiosurgery using the Leksell gamma knife: can FDG PET help to differentiate radionecrosis from tumour progression? *Eur J Nucl Med Mol Imaging*. 2003;30:96–100.

8. Lai G, Mahadevan A, Hackney D, et al. Diagnostic Accuracy of PET, SPECT, and Arterial Spin-Labeling in Differentiating Tumor Recurrence from Necrosis in Cerebral Metastasis after Stereotactic Radiosurgery. *AJNR Am J Neuroradiol*. 2015;36:2250–5.

9. Tomura N, Kokubun M, Saginoya T, et al. Differentiation between Treatment-Induced Necrosis and Recurrent Tumors in Patients with Metastatic Brain Tumors: Comparison among 11C-Methionine-PET, FDG-PET, MR Permeability Imaging, and MRI-ADC-Preliminary Results. *AJNR Am J Neuroradiol*. 2017;38:1520–7.

10. Horky LL, Hsiao EM, Weiss SE, et al. Dual phase FDG-PET imaging of brain metastases provides superior assessment of recurrence versus post-treatment necrosis. *J Neurooncol*. 2011;103:137–46.

11. Matuszak J, Waissi W, Clavier JB, et al. Métastases cérébrales : apport de l'acquisition tardive en TEP/TDM au 18F-FDG pour le diagnostic différentiel entre récurrence tumorale et radionécrose. *Médecine Nucléaire*. 2016;40:196.

12. Bossuyt PM, Reitsma JB, Bruns DE, et al. STARD 2015: An Updated List of Essential Items for Reporting Diagnostic Accuracy Studies. *Radiology*. 2015;277:826–32.

13. Hatzoglou V, Yang TJ, Omuro A, et al. A prospective trial of dynamic contrast-enhanced MRI perfusion and fluorine-18 FDG PET-CT in differentiating brain tumor progression from radiation injury after cranial irradiation. *Neuro Oncol*. 2016;18:873–80.

14. Thust SC, van den Bent MJ, Smits M. Pseudoprogression of brain tumors: Pseudoprogression of Brain Tumors. *J Magn Reson Imaging*. 2018;48:571–89.

15. Derks SHAE, Jongen JLM, van den Bent MJ, et al. Assessment of imaging biomarkers in the follow-up of brain metastases after SRS. *Neuro-Oncology*. 2021;23:1983–4.

16. Landis JR, Koch GG. The Measurement of Observer Agreement for Categorical Data. *Biometrics*. 1977;33:159.

17. Pajak B, Siwiak E, Sołtyka M, et al. 2-Deoxy-d-Glucose and Its Analogs: From Diagnostic to Therapeutic Agents. *IJMS*. 2019;21:234.

18. Chernov M, Hayashi M, Izawa M, et al. Differentiation of the radiation-induced necrosis and tumor recurrence after gamma knife radiosurgery for brain metastases: importance of multi-voxel proton MRS. *Minim Invasive Neurosurg*. 2005;48:228–34.

19. Spence AM, Muzi M, Mankoff DA, et al. 18F-FDG PET of gliomas at delayed intervals: improved distinction between tumor and normal gray matter. *J Nucl Med*. 2004;45:1653–9.

20. Galldiks N, Kocher M, Ceccon G, et al. Imaging challenges of immunotherapy and targeted therapy in patients with brain metastases: response, progression, and pseudoprogression. *Neuro-Oncology*. 2020;22:17–30.

21. Le Rhun E, Guckenberger M, Smits M, et al. EANO–ESMO Clinical Practice Guidelines for diagnosis, treatment and follow-up of patients with brain metastasis from solid tumours. *Annals of Oncology*. 2021;32:1332–47.

22. Okubo S, Zhen H-N, Kawai N, et al. Correlation of L-methyl-11C-methionine (MET) uptake with L-type amino acid transporter 1 in human gliomas. *J Neurooncol*. 2010;99:217–25.

23. Youland RS, Kitange GJ, Peterson TE, et al. The role of LAT1 in (18)F-DOPA uptake in malignant gliomas. *J Neurooncol*. 2013;111:11–8.

24. Wiriyasermkul P, Nagamori S, Tominaga H, et al. Transport of 3-fluoro-L-α-methyl-tyrosine by tumor-upregulated L-type amino acid transporter 1: a cause of the tumor uptake in PET. *J Nucl Med*. 2012;53:1253–61.

25. Yomo S, Oguchi K. Prospective study of 11C-methionine PET for distinguishing between recurrent brain metastases and radiation necrosis: limitations of diagnostic accuracy and long-term results of salvage treatment. *BMC Cancer*. 2017;17:713.

26. Tsuyuguchi N, Sunada I, Iwai Y, et al. Methionine positron emission tomography of recurrent metastatic brain tumor and radiation necrosis after stereotactic radiosurgery: is a differential diagnosis possible? *J Neurosurg*. 2003;98:1056–64.

27. Cicone F, Minniti G, Romano A, et al. Accuracy of F-DOPA PET and perfusion-MRI for differentiating radionecrotic from progressive brain metastases after radiosurgery. *Eur J Nucl Med Mol Imaging*. 2015;42:103–11.

28. Cicone F, Carideo L, Scaringi C, et al. Long-term metabolic evolution of brain metastases with suspected radiation necrosis following stereotactic radiosurgery: longitudinal assessment by F-DOPA PET. *Neuro-Oncology*. 2021;23:1024–34.

29. Galldiks N, Stoffels G, Filss CP, et al. Role of O-(2-(18)F-fluoroethyl)-L-tyrosine PET for differentiation of local recurrent brain metastasis from radiation necrosis. *J Nucl Med*. 2012;53:1367–74.

30. Ceccon G, Lohmann P, Stoffels G, et al. Dynamic O-(2-18F-fluoroethyl)-L-tyrosine positron emission tomography differentiates brain metastasis recurrence from radiation injury after radiotherapy. *Neuro Oncol*. 2017;19:281–8.

31. Romagna A, Unterrainer M, Schmid-Tannwald C, et al. Suspected recurrence of brain metastases after focused high dose radiotherapy: can [18F]FET- PET overcome diagnostic uncertainties? *Radiat Oncol*. 2016;11:139.

32. Heinzel A, Müller D, Yekta-Michael SS, et al. O-(2-18F-fluoroethyl)-L-tyrosine PET for evaluation of brain metastasis recurrence after radiotherapy: an effectiveness and cost-effectiveness analysis. *Neuro-Oncology*. 2017;19:1271–8.

33. Chuang M-T, Liu Y-S, Tsai Y-S, et al. Differentiating Radiation-Induced Necrosis from Recurrent Brain Tumor Using MR Perfusion and Spectroscopy: A Meta-Analysis. Hendrikse J, editor. *PLoS ONE*. 2016;11:e0141438.

34. Kwee RM, Kwee TC. Dynamic susceptibility MR perfusion in diagnosing recurrent brain metastases after radiotherapy: A systematic review and meta- analysis. *J Magn Reson Imaging*. 2020;51:524–34.

35. Huang J, Wang A-M, Shetty A, et al. Differentiation between intra-axial metastatic tumor progression and radiation injury following fractionated radiation therapy or stereotactic radiosurgery using MR spectroscopy, perfusion MR imaging or volume progression modeling. *Magn Reson Imaging*. 2011;29:993–1001.

36. Chernov MF, Hayashi M, Izawa M, et al. Multivoxel proton MRS for differentiation of radiation-induced necrosis and tumor recurrence after gamma knife radiosurgery for brain metastases. *Brain Tumor Pathol*. 2006;23:19–27.

Legends for illustrations:

FIGURE 1.

Flow of participants through the study

Notes: TP, true positive; TN, true negative; FP, false positive; FN, false negative

FIGURE 2.

Three different patients with initially uncharacterized lesions according to contrast-enhanced T1-weighted MRI. Patient (A) was treated by stereotaxic radiotherapy 45 months earlier for a right parietal metastasis of pulmonary carcinoma. Neither standard nor delayed [^{18}F]-FDG PET images showed uptake higher than normal gray matter (Horky's index 0.05). The absence of tumor viability was confirmed by follow-up. Patient (B) had a right occipital metastasis of a head-and-neck carcinoma treated by surgery and stereotaxic radiotherapy 9 months earlier. Whereas the intensity of the lesion was similar to the normal brain on standard [^{18}F]-FDG PET images, delayed images highlighted a focal increased uptake (Horky's index 0.20). Tumor recurrence was proven 21 days later by pathological analysis of resection samples. For the patient (C) who had a right frontal metastasis of breast carcinoma treated with radiation therapy 20 months earlier, standard and delayed [^{18}F]-FDG PET images revealed intense uptake (Horky's index 0.78) and tumor recurrence was confirmed by pathological analysis of resection specimen 47 days after PET.

FIGURE 3.

Box plots showing TBR in radiation necrosis and viable tumors, respectively on standard and delayed [^{18}F]-FDG PET images.

TABLE 1.

Patients' characteristics

TABLE 2.

Diagnostic performance of each method

Supplementary Material.

Positron-emission tomography with computed tomography (PET/CT) systems and protocols used in the three participating centers

Figure 1

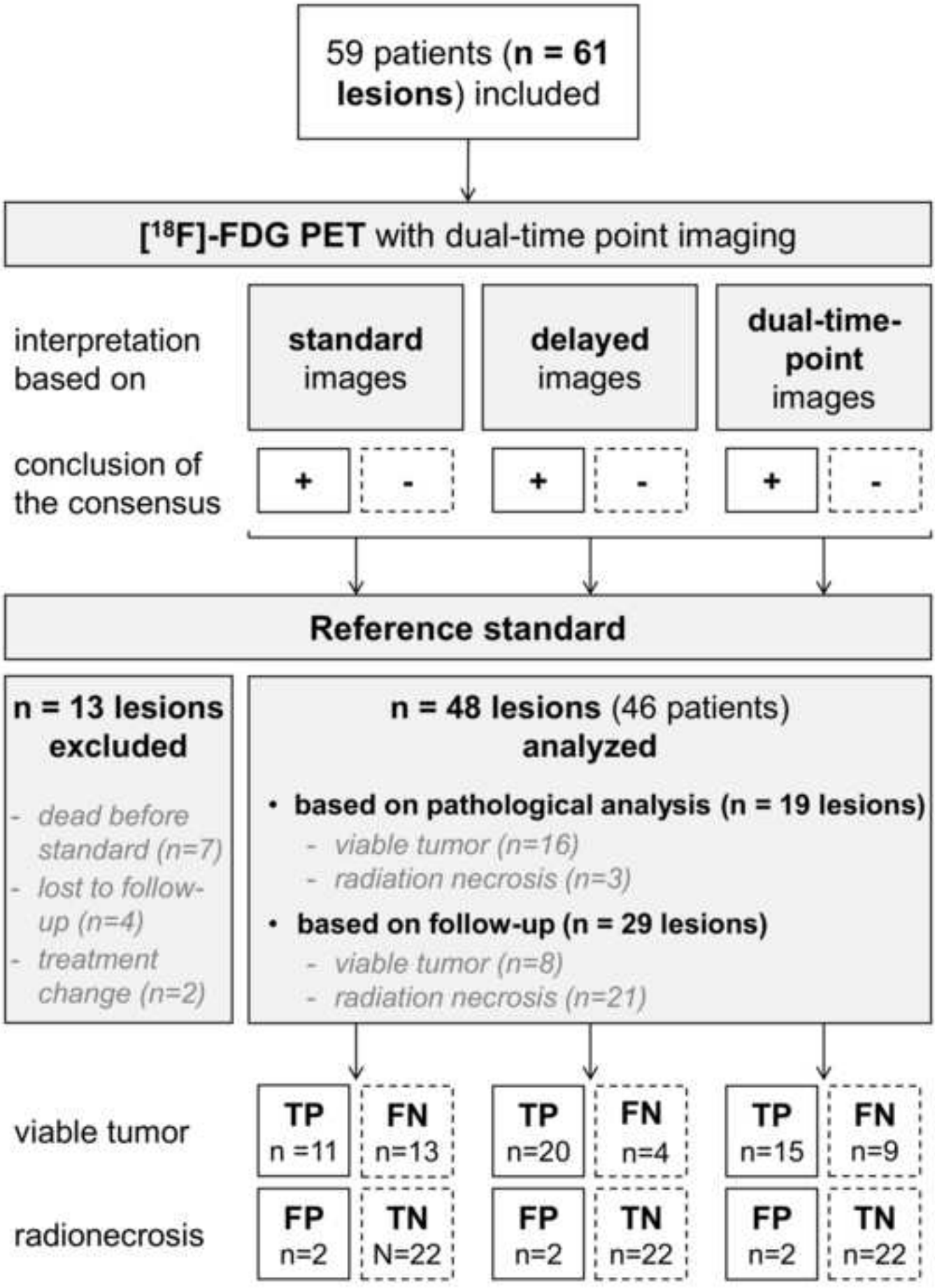

Figure 2

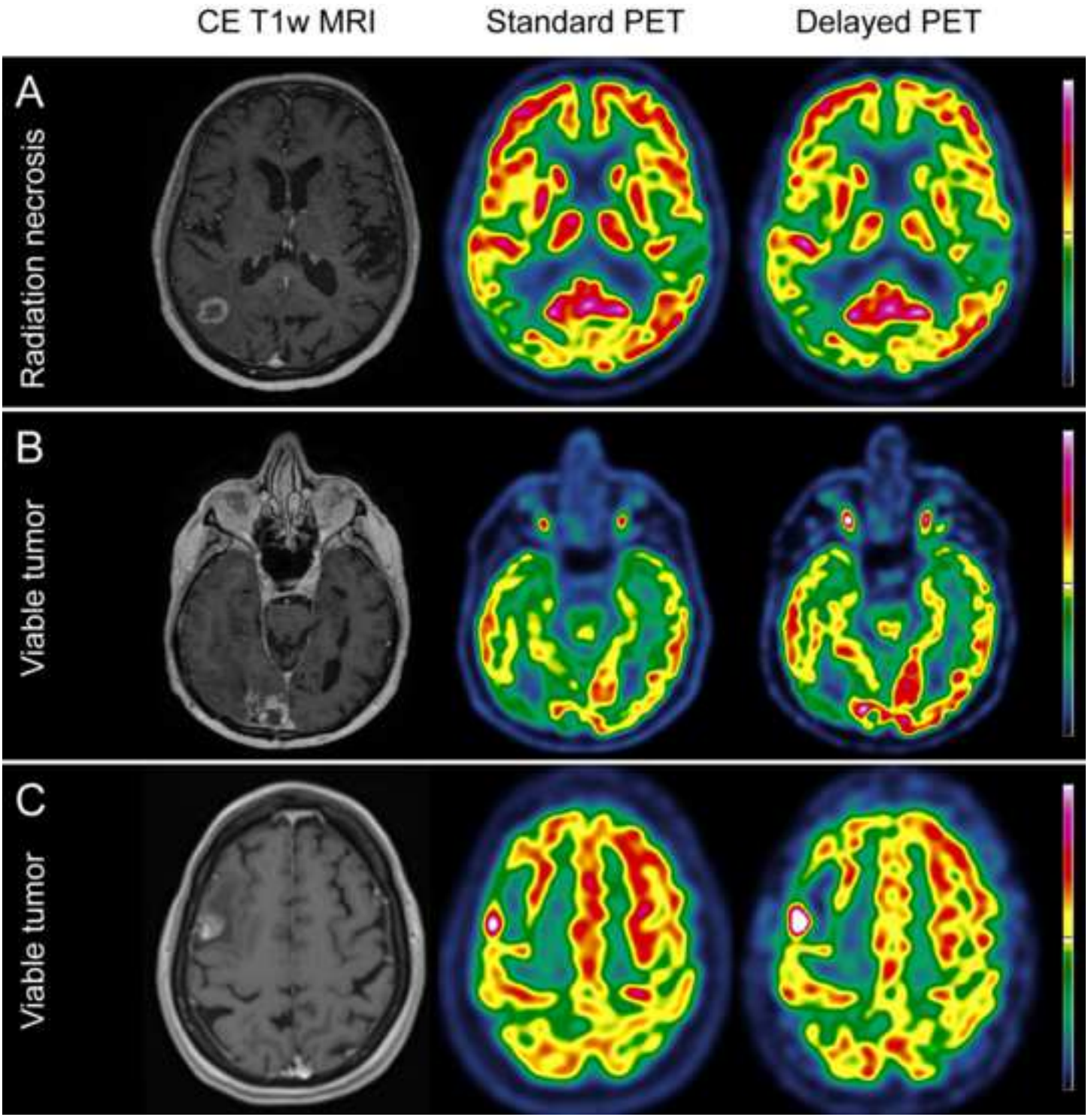

Figure 3

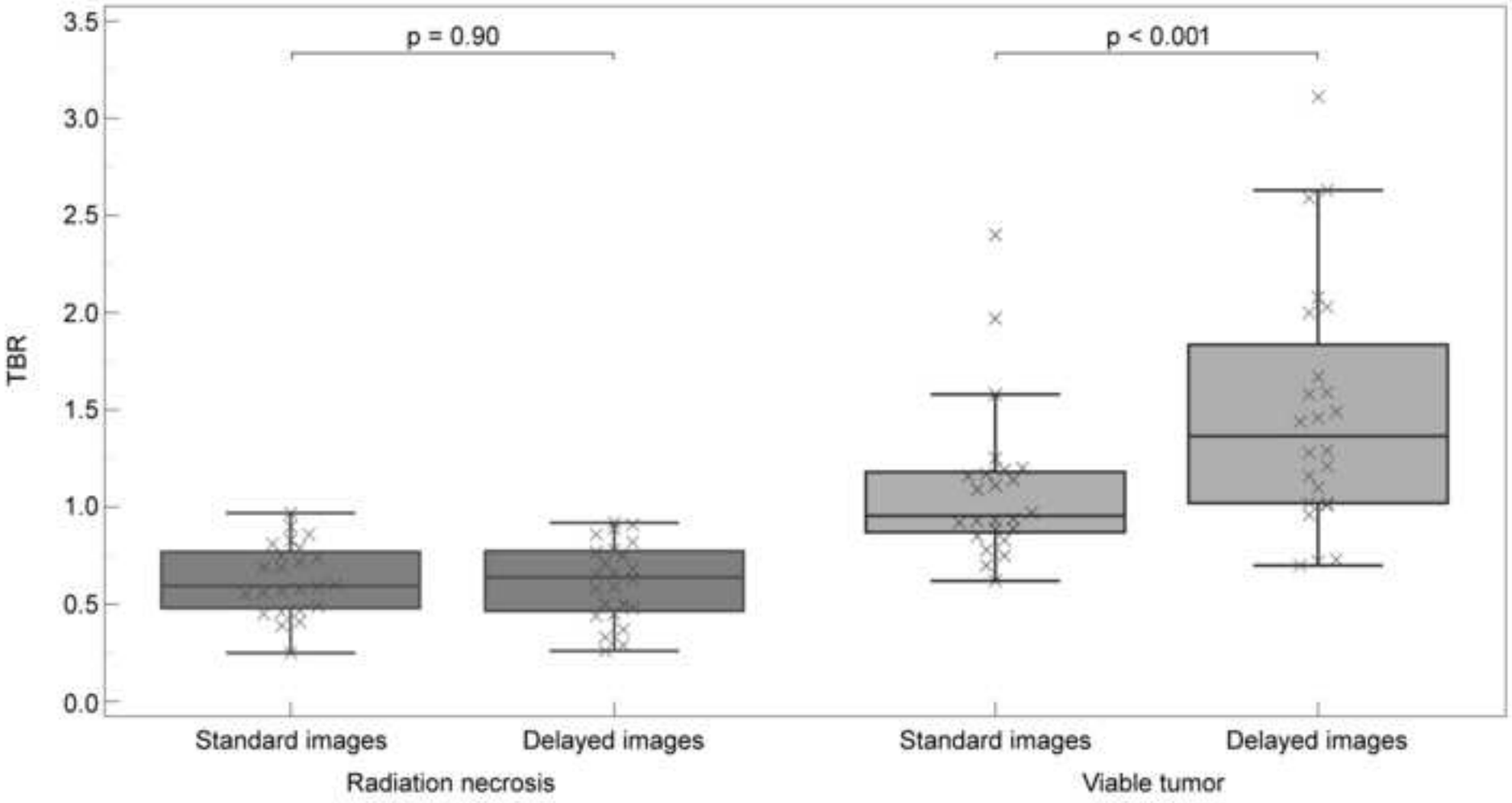

Table 1. Patients' characteristics

	n (%), median [Q1, Q3]
PATIENTS' CHARACTERISTICS (n)	**46**
Age at time of PET (years)	62 [51, 67]
Sex (male / female)	18/28
LESIONS' CHARACTERISTICS (n)	**48**
Primary tumor:	
Lung	27 (57%)
adenocarcinoma	23 (49%)
squamous cells carcinoma	2 (4%)
small cells carcinoma	2 (4%)
Breast	11 (23%)
invasive carcinoma of no special type	9 (19%)
invasive lobular carcinoma	2 (4%)
Digestive	4 (8%)
colon/rectum, adenocarcinoma	3 (6%)
esophagus, adenocarcinoma	1 (2%)
Skin	3 (6%)
melanoma	2 (4%)
squamous cells carcinoma	1 (2%)
Other	3 (6%)
ovary, serous adenocarcinoma	1 (2%)
kidney, clear cell renal cell carcinoma	1 (2%)
head & neck, squamous cells carcinoma	1 (2%)
Laterality: left / right / median	19 (40%) / 28 (58%) /1 (2%)
Location:	
frontal	20 (42%)
parietal	8 (17%)
temporal	7 (14%)
occipital	2 (4%)
cerebellum	11 (23%)
Time delay between MRI and PET (days)	25 [17, 36]
Time delay between radiotherapy and PET (months)	15.7 [9.4, 24.0]
Radiation dose (Gy)	30 [24, 33]
PET: Activity administered (MBq)	201 [197, 229]
PET: injection - acquisition delay (min)	
between injection and standard acquisition (min)	57 [38, 66]
between injection and delayed acquisition (min)	252 [240, 285]
Reference standard:	
pathological analysis	19 (40%)
viable tumor	16 (34%)
radiation necrosis	3 (6%)
imaging and clinical follow-up	29 (60%)
viable tumor	8 (17%)
radiation necrosis	21 (43%)

Table 2

Table 2. Diagnostic performance of each method

	AUC	Sensitivity	Specificity	LR+	LR-	PPV	NPV	Accuracy	Cohen's Kappa
Delayed [^{18}F]-FDG PET images (visual analysis: > healthy gray matter)	0.88 [0.75, 0.95]	0.83 [0.63, 0.95]	0.92 [0.73, 0.99]	10 [2.6, 38.1]	0.18 [0.07, 0.40]	0.91 [0.72, 0.97]	0.84 [0. 69, 0.93]	0.88 [0.75, 0.95]	0.83 [0.68, 0.99]
Standard [^{18}F]-FDG PET images (visual analysis: > healthy gray matter)	0.69 [0.54, 0.81]	0.46 [0.26, 0.67]	0.92 [0.73, 0.99]	5.5 [1.4, 22.2]	0.59 [0.40, 0.90]	0.84 [0.58, 0.96]	0.63 [0.53, 0.71]	0.69 [0.54, 0.81]	0.48 [0.23, 0.74]
Dual-time point (Horky's index: > 0.19)	0.77 [0.63, 0.88]	0.63 [0.41, 0.81]	0.92 [0.73, 0.99]	7.5 [1.9, 29.3]	0.41 [0.20, 0.70]	0.88 [0.66, 0.97]	0.71 [0.59, 0.81]	0.77 [0.63, 0.88]	0.61 [0.38, 0.84]

Notes: Values are presented with their 95% confidence interval. AUC, area under receiver operating characteristics curve; PPV, Positive Predictive Value; NPV, Negative Predictive Value; LR+, Positive Likelihood Ratio; LR-, Negative Likelihood Ratio